DOI: 10.6060/ivkkt.20256801.7096

УДК: 537.525

О ВЛИЯНИИ НАЧАЛЬНОГО СОСТАВА СМЕСИ $CF_4 + CHF_3 + O_2$ НА ПАРАМЕТРЫ ПЛАЗМЫ И КИНЕТИКУ РЕАКТИВНО-ИОННОГО ТРАВЛЕНИЯ КРЕМНИЯ

А.М. Ефремов, А.В. Бобылев, Е.М. Казначеева, K.-H. Kwon

Александр Михайлович Ефремов (ORCID 0000-0002-9125-0763)*

НИИ Молекулярной электроники (НИИМЭ), ул. Академика Валиева, 6/1, Зеленоград, Москва, Российская Федерация, 124460
E-mail: amefremov@mail.ru*

Александр Викторович Бобылев (ORCID 0009-0009-3526-6822)

Ивановский государственный химико-технологический университет, Шереметевский пр., 7, Иваново, Российская Федерация, 153000
E-mail: prototyp16@mail.ru

Екатерина Михайловна Казначеева (ORCID 0009-0006-6976-5900)

Ивановский государственный химико-технологический университет, Шереметевский пр., 7, Иваново, Российская Федерация, 153000
E-mail: katya37light@gmail.com

Kwang-Ho Kwon (ORCID 0000-0003-2580-8842)

Korea University, 208 Seochang-Dong, Chochiwon, Korea, 339-800
E-mail: kwonkh@korea.ac.kr

В работе обсуждаются механизмы влияния соотношения CF_4/CHF_3 в плазмообразующей смеси $CF_4 + CHF_3 + O_2$ на стационарный состав плазмы и кинетику травления кремния в типичных условиях реактивно-ионного процесса. Диагностика плазмы двойным зондом Ленгмюра обеспечивала информацию по электрофизическим параметрам плазмы и предоставляла исходные данные для моделирования кинетики плазмохимических процессов. В результате были подтверждены основные свойства плазмы $CF_4 + O_2$ и $CHF_3 + O_2$, известные из предшествующих работ, а также проведен анализ закономерностей образования и гибели активных частиц в условиях трехкомпонентной смеси. В частности, было обнаружено, что замена CF_4 на CHF_3 при фиксированном содержании кислорода в исходном газе а) вызывает относительно слабые изменения температуры электронов и плотности плазмы; б) приводит к увеличению ее полимеризационной способности; и в) значительно (более чем в 3 раза) снижает концентрацию атомов F. Последний эффект был подтвержден удовлетворительным согласием с экспериментальными данными, полученными с использованием метода оптической эмиссионной актинометрии. В экспериментах по травлению было найдено, что скорость травления кремния снижается от 140 нм/мин до 65 нм/мин с ростом содержания CHF_3. Анализ кинетики травления позволил заключить, что а) доминирующим механизмом травления является ионно-стимулированная химическая реакция; б) эффективная вероятность этой реакции сохраняет практически постоянное значение, несмотря на увеличение скорости фторуглеродной полимерной пленки. Этот эффект может отражать изменение степени пассивации свободной от полимера поверхности атомами кислорода.

Ключевые слова: CF_4, CHF_3, O_2, плазма, параметры, активные частицы, ионизация, диссоциация, травление, полимеризация

Для цитирования:
Ефремов А.М., Бобылев А.В., Казначеева Е.М., Kwon K.-H. О Влиянии начального состава смеси $CF_4 + CHF_3 + O_2$ на параметры плазмы и кинетику реактивно-ионного травления кремния. *Изв. вузов. Химия и хим. технология*. 2025. Т. 68. Вып. 1. С. 39–47. DOI: 10.6060/ivkkt.20256801.7096.

For citation:
Efremov A.M., Bobylev A.V., Kaznacheeva E.M., Kwon K.-H. On effects of initial CF_4 + CHF_3 + O_2 mixture composition on plasma parameters and reactive-ion etching of silicon. *ChemChemTech [Izv. Vyssh. Uchebn. Zaved. Khim. Khim. Tekhnol.]*. 2025. V. 68. N 1. P. 39–47. DOI: 10.6060/ivkkt.20256801.7096.

ON EFFECTS OF INITIAL CF_4 + CHF_3 + O_2 MIXTURE COMPOSITION ON PLASMA PARAMETERS AND REACTIVE-ION ETCHING OF SILICON

A.M. Efremov, A.V. Bobylev, E.M. Kaznacheeva, K.-H. Kwon

Alexander M. Efremov (ORCID 0000-0002-9125-0763)*

Molecular Electronics Research Institute (MERI), Academic Valiev st., 6/1, Zelenograd, Moscow, 124460, Russia
E-mail: amefremov@mail.ru

Alexander V. Bobylev (ORCID 0009-0009-3526-6822)

Ivanovo State University of Chemistry and Technology, Sheremetevskiy ave., 7, Ivanovo, 153000, Russia
E-mail: prototyp16@mail.ru

Ekaterina M. Kaznacheeva (ORCID 0009-0006-6976-5900)

Ivanovo State University of Chemistry and Technology, Sheremetevskiy ave., 7, Ivanovo, 153000, Russia
E-mail: katya37light@gmail.com

Kwang-Ho Kwon (ORCID 0000-0003-2580-8842)

Korea University, 208 Seochang-Dong, Chochiwon, Korea, 339-800
E-mail: kwonkh@korea.ac.kr

In this work, we discussed how the CF_4/CHF_3 ratio in CF_4 + CHF_3 + O_2 gas mixture does influence steady-state plasma composition and silicon etching kinetics in a conventional reactive-ion process. Plasma diagnostics by double Langmuir probes delivered the information on electro-physical plasma parameters and provided input data for the modeling of plasma chemistry. As a result, we confirmed basic properties of CF_4 + O_2 and CHF_3 + O_2 plasmas known from previous works as well as analyzed formation/decay kinetics for plasma active species in the three-component gas mixture. In particular, it was found that the substitution of CF_4 by CHF_3 at fixed content of oxygen in a feed gas a) causes weak changes in electron temperature and plasma density; b) leads to an increase in plasma polymerizing ability; and c) sufficiently (by more than 3 times) reduces F atom density. The last effect was confirmed by the satisfactory agreement with experimental data obtained using the optical emission actinometry method. Etching experiments indicated a monotonic decrease in Si etching rate toward CHF_3-rich plasmas, from 140 nm/min down to 65 nm/min. The analysis of etching kinetics allowed one to conclude that a) the dominant etching mechanisms is the ion-assisted chemical reaction; and b) the effective reaction probability keeps the nearly constant value, in spite of increasing polymer deposition rate. This effect may reflect the change in passivation of polymer-free surface by oxygen atoms.

Keywords: CF_4, CHF_3, O_2, plasma, parameters, active species, ionization, dissociation, etching, polymerization

INTRODUCTION

Reactive-ion etching (RIE) of silicon and silicon-based materials in fluorocarbon gas plasmas are key steps of modern micro- and nano-electronics technology, as these determine both feature sizes and functional characteristics for integrated components [1-3]. The widely used RIE tool is the inductively-coupled plasma (ICP) etching systems which operate with two power sources and thus, allow one to adjust independently active species fluxes and ion bombardment energy [1, 4]. Therefore, the possibility to control the balance between physical and chemical etching pathways enlarges the available range of output RIE characteristics (etching rate, etching selectivity in respect to mask material and etching profile shape) as well as helps to achieve the advanced device structure and performance [4-6].

From many previous studies related to fluorocarbon gas plasmas, it can be understood that the overall RIE result strongly depends on the polymerizing ability of given fluorocarbon gas. Corresponding property is directly coupled with “F/C” (fluorine to carbon atom) ratio in the original fluorocarbon molecule (in fact, with the relation between densities of F atoms and polymerizing CF_x radicals) as well as appears to be stronger in the presence of hydrogen [4, 7, 8]. The latter is probably due to higher sticking coefficients and polymer chain formation probabilities for CH_x species compared with CF_x ones. For instance, the CF_4 plasma is featured by [F] >> [CF] + [CF_2] under typical RIE conditions [9, 10] as well as exhibits the minimum polymerizing ability among other fluorocarbons [7, 11]. Such situation pre-determines high Si etching rates with low etching residues, but produces the nearly isotropic etching profile and low SiO_2/Si etching selectivity [11, 12]. At the same time, its “closest relative” CHF_3 exhibits somewhat opposite properties, as it is characterized by the domination of CF_x and CHF_x over F species in a gas phase [9, 13]. As a result, the deposition of thick fluorocarbon polymer film lowers absolute etching rates, increases surface residues, provides more anisotropic etching (due to the protective effect of polymer film on side walls) [10, 11] and causes the much better SiO_2/Si etching selectivity (due to the thinner polymer film and the better access of F atoms to the oxygen-containing surface) [12].

The known method to set the etching/polymerization balance according to given process requirements is to combine the fluorocarbon gas with additive component which suppresses or enforces the polymerization [1, 3, 4]. In particular, the addition of O_2 oxidizes CF_x radicals into non-polymerizing CF_xO and CO_x compounds, causes an increase in F atom density as well as promotes the oxidative destruction of deposited polymer film [4, 14, 15]. In our previous works [16-18], we have studied basic properties of $CF_4 + O_2$ and $CHF_3 + O_2$ plasmas as well as compared the etching kinetics of silicon under identical processing conditions. The common features were that the transition toward O_2-rich gas mixtures a) disturbs electro-physical plasma parameters; b) initiates $CF_x + O/O(^1D) \rightarrow$ $\rightarrow CF_{x-1}O + F$ reactions pathways that rapidly (by more than an order of magnitude at 0-50% O_2) lowers densities of fluorocarbon radials; c) causes the non-monotonic (with maximum values at ~ 30% O_2 in CF_4-based plasma and ~ 50% O_2 in CHF_3-based plasma [17]) behavior of F atom density; and d) lowers the reaction probability of F atoms with the polymer-free Si surface. Concerning the last phenomenon, suggested mechanisms are the transformation of reaction product into lower volatile SiF_xO_y compounds and/or the oxidation of silicon itself [15-17]. As such, there is a need to have another method for adjusting the etching/polymerization balance where above effects will remain on the minimum level.

The general aim of this work was to investigate how the ratio of fluorocarbon components in CF_4 + + CHF_3 + 50% O_2 gas mixture does influence gas-phase plasma characteristics and features of Si etching process. Accordingly, the main attention was focused on corresponding changes in electrons- and ions related plasma parameters, kinetics and densities of both fluorine atoms and polymerizing radicals as well as in heterogeneous kinetic coefficients characterizing the interaction of F atoms with Si surface.

EXPERIMENTAL AND MODELING DETAILS

Experimental setup and conditions

Experiments were carried out in the planar inductively coupled plasma (ICP) reactor, the same as was used in our previous works [15-19]. Schematic diagram of reactor environment as well as the detailed description of experimental setup may be found in Refs. [15, 17]. Plasma was excited using the 13.56 MHz rf generator connected to the flat coil on the top side of reactor chamber. Both input power (W_{inp}) and total gas pressure (p) were constant and fixed at 700 W and 6 mtor, respectively. Another 13.56 MHz rf source powered the chuck electrode to control the ion bombardment energy (ε_i) through the change in the negative dc bias voltage ($-U_{dc}$). As the bias power (W_{dc}) was also kept on the constant level of 200 W, the parameter $-U_{dc}$ was slightly sensitive to the ion flux coming from the bulk plasma. The initial composition of $CF_4 + CHF_3 + O_2$ gas mixture was set by adjusting partial flow rate for component gases within the total flow rate q = 40 sccm. In order to characterize the content of components in a feed gas, we used their relative concentrations (or mole fractions) y_i found as $(q_i/q) \times 100\%$. In particular, the constant $q(O_2)$ = 20 sccm always provided $y(O_2)$ = 50% while the other half was composed by different values of $y(CF_4)$ and $y(CHF_3)$. Accordingly, an increase in $q(CHF_3)$ from 0-20 sccm corresponded to $y(CHF_3)$ = 0-50%, or to the full substitution of CF_4 by CHF_3.

For etching experiments, we used fragments of standard Si (111) wafer with an average size of ~ 2×2 cm. Etched samples were located in the middle part of chuck electrode, and the latter was thermally stabilized at ~ 20 °C using the water-flow cooling system. After the exposure in plasma, the etched depth Δh was measured using the surface profiler (Alpha-Step 500, Tencor). For this purpose, we provided a partial surface masking by the photoresist AZ1512 with a thickness of

~ 1.5 μm. Preliminary, it was found that the dependence of Δh on processing time exhibits the nearly linear shape up to τ = 10 min. Therefore, assuming the steady-state etching regime, the Si etching rate was simply calculated as $R = \Delta h/\tau$ for τ = 1 min. It is important to note also that the small sample size was especially selected to exclude the loading effect as well as to minimize the disturbance of gas-phase plasma characteristics by etching products. As a result, we obtained no differences in both Si etching rates and plasma diagnostics data obtained with and without sample loading as well as with simultaneous loading of several samples.

Plasma diagnostics procedures

Plasma diagnostics was represented by double Langmuir probe (LP) measurements (DLP2000, Plasmart Inc.) and optical emission spectroscopy (OES) (AvaSpec-3648, JinYoung Tech).

In LP measurements, the probe head was installed through the viewport on the chamber wall as well as was centered in the radial direction. In order to minimize experimental errors due to the deposition of fluorocarbon polymer on probe tips, these were conditioned in 50% Ar + 50% O_2 plasma for ~ 5 min before and after each measurement. Such procedure provided the decent similarity in both raw current-voltage (I-V) curves and related plasma parameters obtained in a series of independent measurements under identical processing conditions. The treatment of I-V curves was based on well-known statements of Langmuir probe theory for low-pressure high-density plasmas [4, 20]. As a result, data on electron temperature (T_e) and ion current density (J_+) were available.

In OES measurements, the plasma emission spectra were investigated through the quarts window which sealed the viewport instead of Langmuir probe tool. In order to obtain information on F atom density, we fulfilled the $CF_4 + CHF_3 + O_2$ gas mixture by 2 sccm (~ 4.5%) of Ar as well as monitored intensities (I) for F 703.8 nm (ε_{th} = 14.75 eV) and Ar 750.4 nm (ε_{th} = 13.48 eV) emission maxima. As corresponding atomic lines exhibit low radiative lifetimes and direct electron-impact excitation with accurately known cross-sections [21], their combination represents the well-known actinometry couple used by many researches. Accordingly, the standard actinometrical approach [21, 22] yields

$$[F] = y_{Ar} N C_a (I_F/I_{Ar}), \quad (1)$$

where y_{Ar} is the Ar fraction in a feed gas, $N = p/k_B T_{gas}$ is the total gas density at the gas temperature of T_{gas}, and $C_a = (\lambda_{Ar} k_{ex,F} A_F)/(\lambda_F k_{ex,Ar} A_{Ar})$ is the actinometrical coefficient that depends on corresponding wavelengths (λ), excitation rate coefficients (k_{ex}) and optical transition probabilities (A). In Ref. [21], it was shown that $C_a \approx 2.0$ at T_e = 3-6 eV. Similarly to our previous works [15-19], we assumed T_{gas} be independent on gas mixing ratio and equal to ~ 600 K. The latter is quite typical for ICP reactors of given geometry operated at power densities of ~ 0.5 W/cm^3 [23]. In a series of preliminary experiments, it was found also that the presence of Ar does not influence plasma parameters, and thus does not disturb the F atom kinetics. Therefore, F atom densities obtained from Eq.(1) may surely be equalized with those in Ar-free plasmas.

In both etching and plasma diagnostics experiments, each point corresponded to the given set of processing conditions was repeated by 5 times, while the data were averaged before their plotting and/or tabulating. Typical deviations in respect to average values were about 5% in LP and OES measurements as well as were always below 10% in the case of etched depth.

Plasma modeling

In order to obtain the information on densities and fluxes of plasma active species, we applied a simplified 0-dimensional (global) model operating with volume-averaged plasma parameters. The kinetic scheme (the list of reactions with related rate coefficients) was constructed from those suggested in previous works for modeling of CF_4 + Ar/O_2 and CHF_3 + + Ar/O_2 [13, 14, 17, 24] plasmas. As in both cases authors reported the satisfactory agreement between measured and model-predicted plasma parameters, the discussion about the content of kinetic scheme was not the subject of given study. Modeling algorithm accounted for a set of typical approaches reflecting the features of low-pressure ($p < 20$ mtor) high-density ($n_+ > 10^{10}$ cm^{-3}, where n_+ is the total ion density) inductive discharges [4]. In particular, it was assumed that

1. The electron energy distribution function (EEDF) has the nearly Maxwellian shape. Physically, such situation is provided by the sufficient contribution of equilibrium energy exchanges in electron-electron collisions. Accordingly, rate coefficients for electron-impact reactions may be obtained in a form of fitting expressions $k = f(T_e)$ [14, 24, 25].
2. The low electronegativity of CF_4, CHF_3 and O_2 gases results in $n_e \approx n_+$, where n_e is the electron density [10, 13, 14, 24, 25]. The reasons are the high ionization degree for gas species ($n_+/N > 10^{-4}$) as well as the low efficiency of dissociative attachment processes at low pressures. All these reveal $J_+ \approx 0.61 e n_+ (eT_e/m_i)^{1/2}$ [4], where m_i is the effective (ion-type-averaged) ion mass. The latter may be evaluated through individual masses and fractions of dominant positive ions, as was described in Refs. [15, 17].

3. The loss of atoms and radicals on chamber walls follows the first-order recombination kinetics with nearly constant reaction probabilities [15, 17]. The latter is because of the nearly constant internal wall temperature, as can be expected from the negligible change in the temperature of external wall.

The input model parameters were experimental data on T_e and J_+ obtained by LP plasma diagnostics at different CF_4/CHF_3 mixing ratios. As outputs, the model provided steady-state densities and fluxes for both charged and neutral ground-state species.

RESULTS AND DISCUSSION

When analyzing the influence of CF_4/CHF_3 mixing ratio on electrons- and ions-related plasma parameters (Table 1), it was concluded that corresponding phenomena a) surely reflect differences between CF_4- and CHF_3- based plasmas diluted by 50% O_2, as shown in Refs. [16, 17]; and b) have reasonable interpretations with accounting for model-predicted plasma composition (Fig. 1). Accordingly, most important findings may briefly be explained as follows:

– The noticeable growth of electron temperature at W = const definitely points out on lower in electron energy losses in CHF_3-rich plasmas. Really, from Fig. 1(a), it can be seen that an increase in $y(CHF_3)$ causes the substitution of dominant molecular component CF_2O by HF molecules. As the latter exhibits the diatomic structure and the lower size compared with that for CF_2O, one can reasonably suggest also lower cross-sections for vibrational excitation, electronic excitation and ionization. Accordingly, an increase in [HF] together with $y(CHF_3)$ suppresses electron energy losses in both elastic and inelastic collisions, increases the fraction of high-energy electrons in EEDF as well as causes the growth of their mean energy, $3/2T_e$.

– A weak increase in plasma density is mainly provided by increasing total ionization frequency, $\nu_{iz} \approx k_1[F] + k_2[F_2] + k_3[CF_2O] + k_4[HF]$, where "k" are rate coefficients for R1: $F + e \rightarrow F^+ + 2e$, R2: $F_2 + e \rightarrow F_2^+ + 2e$, R3: $CF_2O + e \rightarrow CF_2O^+ + 2e$ and R4: $HF + e \rightarrow HF^+ + 2e$. Such situation is because the condition of $k_4 < k_1 \approx k_2 \approx k_3$ is overcompensated by the growth of all ionization rate coefficients together with T_e, so that $\nu_{iz} \approx 1.9\times10^4$–$3.2\times10^5$ s^{-1}, or by ~ 1.6 times for 0–50% CHF_3. The weaker effect on both n_+ and n_e (by ~ 1.2 times for 0-50% CHF_3) is because of the acceleration of their transport to chamber walls due to an increase in electron diffusion coefficient and ion Bohm velocity. Accordingly, similar tendencies for ion flux Γ_+ (5.8×10^{15}–7.8×10^{15} $cm^{-2}s^{-1}$ at 0-50% CHF_3) and ion current density $J_+ \approx e\Gamma_+$ also take place.

– A relative decrease in the ion bombardment energy (as follows from the behavior of $-U_{dc}$) appears to be weaker compared with that for Γ_+, so that the parameter $G1 = (M_i\varepsilon_i)^{1/2}\Gamma_+$, where $M_i = N_A m_i$, keeps an increasing tendency toward CHF_3-rich plasmas. As the latter characterizes the ion bombardment intensity [15-17], one can expect the somewhat acceleration of ion-driven heterogeneous processes.

Table 1

Electrons- and ions-related plasma parameters

***Таблица 1.* Параметры электронной и ионной компонент плазмы**

$y(CHF_3)$, %	T_e, eV	J_+, mA/cm^2	$n_+ \approx n_e$, 10^{10} cm^{-3}	$-U_{dc}$, V	G1, 10^{17}
0	3.8	0.93	3.02	280	6.13
25	4.2	1.12	3.39	266	7.07
50	4.5	1.24	3.53	255	7.53

Note: $G1 = (M_i\varepsilon_i)^{1/2}\Gamma_+$ ($eV^{1/2}cm^{-2}s^{-1}$)

Примечание: $G1 = (M_i\varepsilon_i)^{1/2}\Gamma_+$ (eB$^{1/2}$см$^{-2}$с$^{-1}$)

The chemistry of neutral species in CF_4 plasma in the absence of oxygen has been studied by several authors using both experimental and modeling methods [10, 13, 26, 27]. When summarizing corresponding data obtained at conventional RIE conditions, the basic features of plasma composition and F atom kinetics can be formulated as follows. First, the dominant formation pathways for F atoms are R5: $CF_x + e \rightarrow CF_{x-1} + F + e$ for x = 4 and R6: $CF_4 + e \rightarrow CF_3^+ + F + 2e$. Therefore, as both reactions also produce CF_3 radicals, the condition of $[F] \approx [CF_3]$ surely takes place. Second, the stepwise formation of CF_x species in R5 reaction family lowers their densities with decreasing "x" value. That is why the rule of $[CF_x] > [CF_{x-1}]$ always does work. And thirdly, the loss of F atoms and CF_x radicals is mainly due to their recombination on chamber walls in R7: $F + CF_x \rightarrow CF_{x+1}$ and R8: $F + F \rightarrow F_2$. As the last process produces the noticeable amount of F_2 molecules, their dissociation in R9: $F_2 + e \rightarrow 2F + e$ brings about 10% to the total F atom formation rate. Such situation is also due to the low threshold energy (~ 4.3 eV for R9 compared with ~ 5.6 eV for R5 (x = 4) and ~15.9 eV for R6) that results in $k_9 > k_5$ and k_6.

The dilution of CF_4 by O_2 enriches the gas phase by active oxygen atoms due to R10: $O_2 + e \rightarrow O/O(^1D) + e$ as well as causes the oxidation of CF_x radicals into CF_2O, CFO, CO and CO_2 species in R11: $CF_x + O/O(^1D) \rightarrow CF_{x-1}O + F$. The results are the rapid (by more than two orders of magnitude at 0-50% O_2) decrease in densities of CF_x radicals as well as the domination of CF_2O molecules among over molecular species (Fig. 1). Except the work of R11, the last phenomenon is also contributed by the effective formation

of CF_2O species in R12: 2CFO → CF_2O + CO, R13: CFO + F → CF_2O and R14: CFO + CF_x → CF_2O + + CF_{x-1}. Another important effect is the sufficient growth of F_2 density due to the powerful add-on to their formation rate from the side of R15: CF_2O + O/O(^{1}D) → → F_2 + CO_2. As a result, the leading impact to the production of F atoms is transferred to R9, R16: CF_xO + e → $CF_{x-1}O$ + F + e, R17: FO + e → F + O + e, R18: F_2 + O/O(^{1}D) → FO + F, R19: FO + O/O(^{1}D) → O_2 + F and R20: CFO + O/O(^{1}D) → CO_2 + F. As all these causes an increase in the total fluorine atom formation rate, the same change in their density compared with non-oxygenated plasma also takes place. Therefore, our model-predicted data surely confirmed results of several previous works dealt with CF_4 + O_2 plasmas [14, 16, 17].

The substitution of CF_4 by CHF_3 promotes the formation of CF_x (x = 1, 2) radicals (as the dominant electron-impact dissociation channel for various CHF_x species is R21: CHF_x + e → CF_x + H + e) as well as introduces the new channel for the loss of F atoms in a form of R22: CHF_x + F → CF_x + HF. The latter lifts up the total F atom loss frequency as well as results in sufficiently decreasing [F] value, as shown in Fig. 1(a). Another important phenomenon is that R22 and R23: CF_x + H → CF_{x-1} + HF provide the effective conversion of CHF_x and CF_x species into HF molecules. As a result, these become to be the main gas-phase component starting from 35-40% CHF_3 while partial densities of CHF_x family appear to be below 10^{10} cm^{-3}. It is important to note also that reaction R24: HF + O → F + OH has the high energy threshold (as the strength of H-F bond ~ 570 kJ/mol is higher than ~ 430 kJ/mol for H-O one [28]) and exhibits the extremely low rate coefficient at gas temperatures below 1000 K [29]. That is why the weak increase in O atom density is due to the combined effect from increasing efficiency of R10 and decreasing rate of R18 that follows the change in F_2 density. As a result, the simultaneous increase in densities of CF_2, CF and O species produces the synergetic effects on CO and CFO molecules (Fig. 1(b)). Data of Fig. 2 indicate also that F atom densities provided by our model are in the satisfactory agreement with those resulted from the actinometry experiments. Taking into account that the multi-channel reaction scheme closely matches calculated [F] values with kinetics of other species, one can assume the correct model-based description of main kinetic effects determining the steady-state composition of CF_4 + CHF_3 + O_2 plasma.

In order to evaluate how above changes in plasma composition do influence its polymerizing ability, one can account for the set of tracing parameters suggested in our previous works [16, 17]. These were based on numerous studies of heterogeneous processes kinetics in polymerizing plasmas summarized in Refs. [4, 7, 11, 12, 30]. In particular, the growth of fluorocarbon polymer film is provided by CH_xF_y (x + y < 3) radicals and appears to be faster in fluorine-poor plasmas. The latter is because F atoms saturate free bonds on the plasma/polymer interface and thus, decrease the sticking probabilities for radicals coming from a gas phase. Therefore, the change in the polymer deposition rate may be traced by the parameter G2 = Γ_{pol}/Γ_F, where Γ_F is the flux of F atoms, and Γ_{pol} is the total flux of polymerizing radicals composed by CF_2, CF and CHF. In addition, parameters G3 = G2/G1 and G4 = = G2/Γ_O, where Γ_O is the oxygen atom flux, characterize relative changes in polymer film thickness due to physical sputtering and etching by O atoms, respectively. From Tab. 2, it can be seen that the substitution of CF_4 by CHF_3 increases the total flux of polymerizing radicals (mostly due to an increase in CF and CF_2 densities, as shown in Fig. 1(b)) as well as causes the growth of polymer deposition rate. As the latter appears to be faster (by ~ 25 times at 0–50% CHF_3) compared with an increase in both ion bombardment intensity (by ~ 1.2 times at 0–50% CHF_3) and O atom flux (~ 1.3 times at 0–50% CHF_3), an increase in the polymer film thickness surely takes place. In other words, an increases in y(CHF_3) results in increasing plasma polymerizing ability. The similar phenomenon was reported in our previous work dealt with CF_4 + CHF_3 + + Ar plasma [30].

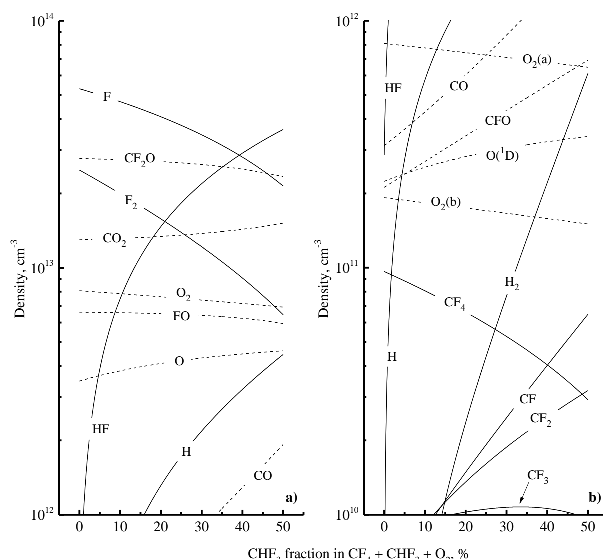

Fig. 1. Model-predicted densities of neutral species as functions of CHF_3 fraction in a feed gas. Dashed lines are to highlight oxygen-containing components

Рис. 1. Расчетные концентрации нейтральных частиц в зависимости от доли CHF_3 в плазмообразующем газе. Пунктирными линиями выделены кислородсодержащие компоненты

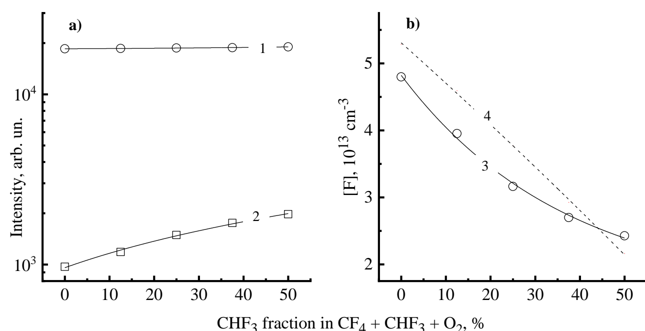

Fig. 2. Emission intensities for F 703.8 nm (1) and Ar 750.4 nm (2) lines as well as F atom density obtained after the actinometry procedure (3) as functions of CHF_3 fraction in a feed gas. Dashed line (4) in Fig. b) repeats the model-predicted F atom density from Fig. 1

Рис. 2. Интенсивности излучения линий F 703,8 нм (1) и Ar 750,4 нм (2), а также концентрации атомов фтора, полученные методом актинометрии (3), в зависимости от доли CHF_3 в плазмообразующем газе. Пунктирная линия (4) на рис. b) дублирует расчетную концентрацию атомов фтора с рис. 1

Table 2

Gas-phase parameters to trace etching and polymerization kinetics

Таблица 2. **Параметры газовой фазы, отслеживающие кинетику травления и полимеризации**

y(CHF_3), %	Γ_{pol}, 10^{16} cm^{-2}s^{-1}	G2, 10^{-2}	G3, 10^{-20}	G4, 10^{-19}	G5
0	0.02	0.01	0.02	0.02	1.91
25	0.06	0.07	0.09	0.07	1.18
50	0.17	0.36	0.47	0.28	0.63

Note: G2 = Γ_{pol}/Γ_F; G3 = G2/G1 (eV$^{-1/2}$cm^{2}s); G4 = G2/Γ_O (cm^{2}s); and G5 = Γ_F/G1 (eV$^{-1/2}$)

Примечание: G2 = Γ_{pol}/Γ_F; G3 = G2/G1 (эВ$^{-1/2}$см^{2}с); G4 = G2/Γ_O (см^{2}с); and G5 = Γ_F/G1 (эВ$^{-1/2}$)

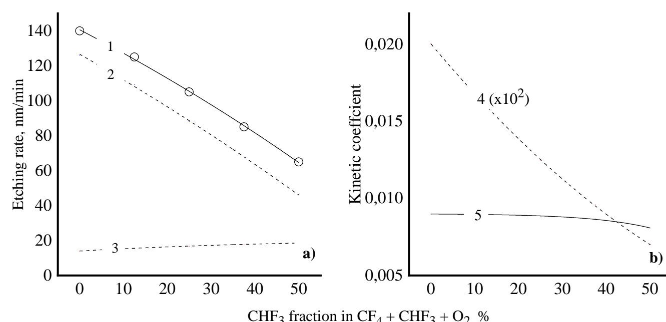

Fig. 3. Silicon etching rate (1–3) and kinetic coefficients characterizing heterogeneous stages of etching process (4, 5) as functions of CHF_3 fraction in a feed gas. In Fig. a): 1 – measured etching rate; 2 – rate of ion-assisted chemical reaction, R_{chem}; and 3 – rate of physical sputtering, R_{phys}. In Fig. b): 4 – etching yield, Y_R; and 5 – effective reaction probability, γ_R

Рис. 3. Скорость травления кремния (1–3) и кинетические коэффициенты (4, 5), характеризующие гетерогенные стадии процесса травления, в зависимости от доли CHF_3 в плазмообразующем газе. На рис. a): 1 – измеренная скорость травления; 2 – скорость ионно-стимулированной химической реакции, R_{chem}; и 3 – скорость физического распыления, R_{phys}. На рис. b): 4 – выход травления, Y_R; и 5 – эффективная вероятность химической реакции, γ_R

From etching experiments, it was found that measured Si etching rate decreases monotonically and almost linearly with increasing CHF_3 fraction in a feed gas (Fig. 3(a)). The mentioned tendency is opposite to the change in ion bombardment intensity (as the latter demonstrates the weak growth toward CHF_3-rich plasmas, see Table 1), but repeats the behavior of F atom flux. Formally, such situation points out on the domination of chemical etching pathway.

From Refs. [4, 17, 30], it can be understood that measured etching rate, R, represents the superposition of partial rates of physical sputtering (R_{phys}) and ion-assisted chemical reaction (R_{chem}). The noticeable role of R_{chem} in or case directly follows from absolute values of process yield calculated as $Y_R = R/\Gamma_+$ (Fig. 3(b)). Obviously, the range of 2.0-0.7 atom/ion at ε_i = 303-282 eV is abnormally high compared with typical Si sputter yields in chemically inert gas environments, Y_S (for example, $Y_S \approx 0.2$ atom/ion at ion energies of ~ 300 eV, as follows from Refs. [31]). In order to divide contributions of physical and chemical etching pathways, we determined the physical etching component as $R_{phys} = Y_S\Gamma_+$, and then, found $R_{chem} = R-R_{phys}$. The result was that R_{phys} increases slightly (14-19 nm/min for 0-50% CHF_3) following the behavior of G1 while R_{chem} demonstrates the deep decrease (126-46 nm/min for 0-50% CHF_3) with keeping the condition of $R_{chem} \gg R_{phys}$. The latter suggests that the main etching mechanism determining the overall process kinetics is heterogeneous chemical reaction represented by a consequence of R25: Si(s.) + xF → SiF_x(s.) and R26: SiF_x(s.) → SiF_x. As the last process appears spontaneously due to the high volatility of saturated SiF_4 compounds even at nearly room temperatures [4], the limiting stage may surely be related to R25. Another important finding was that a decrease in R_{chem} (by ~ 2.7 times for 0-50% CHF_3) almost completely corresponds to the change in F atom flux that points out on the nearly constant effective reaction probability for R25, $\gamma_R = R_{chem}/\Gamma_F$ (Fig. 3(b)). From previously published works, it can be understood that the effective probability for the reaction of F atoms with silicon in oxygen-containing fluorocarbon gas plasmas is sensitive to two main factors, such as a) plasma polymerizing ability (as the thicker polymer film may retard the transport of F atoms to the etches surface) [4, 11, 12]; and b) the oxygen-related heterogeneous effects initiated by the competitive adsorption of oxygen atoms [16, 17]. In our opinion, the first mechanism does not work because γ_R does not "feel" the sufficient increase in both polymer deposition rate and polymer deposition/decomposition rate ratio, as follows from data of Tab. 2. Obviously, such

situation may take place only if the given amount of oxygen provides the effective destruction of polymer film, so that the latter exhibits either the very low thickness or the non-continuous island-like structure. As for the second mechanism, it looks quite possible, especially taking into account the evident agreement between weakly decreasing γ_R and weakly increasing O atoms flux. The latter follows from corresponding change in O atom density shown in Fig. 1. From chemical point of view, one can imagine that the competitive adsorption of O atoms leads to either oxidation of silicon itself R27: Si(s.) + xO → SiO_x(s.) or the conversion of etching products into lower volatile compounds R28: SiF_x(s.) + yO → SiF_xO_y(s.). All these assume the appearance of ion-assisted stages R29: SiO_x(s.) → → SiO_{x-1}(s.) + O and R30: SiF_xO_y(s.) → SiF_xO_y as well as results in decreasing fraction of free adsorption sites for F atoms. It is important to note that exactly same reaction mechanisms were found to be most reasonable to explain the behavior of γ_R in oxygen-rich CF_4 + O_2 and CHF_3 + O_2 plasmas under almost identical processing conditions [17]. The similarity of corresponding phenomena reveals that we probably found correct matching between gas-phase chemistry and heterogeneous process kinetics in oxygenated fluorocarbon gas plasmas.

Finally, we would like to focus the attention on the parameter G5 = Γ_F/G1 which traces the balance between directional and chaotic etching pathways as well as characterizes the etching anisotropy. From Tab. 2, it can be seen that am increase y(CHF_3) results in decreasing G5 (by ~ 3 times at 0-50% CHF_3) that means the transition to more anisotropic etching. Therefore, the CF_4/CHF_3 mixing ratio seems to be the additional tool to adjust the shape of etching profile. At the same time, the direct confirmation by experiments is required.

CONCLUSIONS

This work dealt with CF_4 + CHF_3 + O_2 gas mixture as well as was focused on relationships between CF_4/CHF_3 mixing ratios, steady-state densities of plasma active species and silicon etching kinetics. Plasma diagnostics by double Langmuir probes in combination with 0-dimensional (global) plasma model indicated that the substitution of CF_4 by CHF_3 at constant fraction of oxygen in a feed gas a) does not lead to principal changes in electron temperature and plasma density (due to no principal changes in electron energy loss channels and total ionization rate); b) causes an increase in plasma polymerizing ability (due to increasing densities and fluxes of polymerizing radicals); and c) reduces F atom density (due to an increase in their loss frequency in CHF_x + F → CF_x + HF reaction family. The last effect (and thus, the general reasonability of plasma modeling results) was confirmed by satisfactory agreement with F atom densities measured by optical emission actinometry using the F 703.8 nm/Ar 750.4 nm intensity ratio. The analysis of Si etching kinetics with model-predicted fluxes of plasma active species allowed one to conclude that a) the dominant etching mechanisms are the ion-assisted chemical reaction that composes more than 70% of total etching rate; and b) the nearly-constant effective reaction probability does not correlate with increasing polymer deposition rate, as it normally takes place in polymerizing plasmas in the absence of oxygen. In our opinion, such situation reflects the change in passivation of polymer-free surface by oxygen atoms.

The work was supported by the Ministry of Higher Education and Science of the Russian Federation, project no. FZZW-2023-0010.

The authors declare the absence a conflict of interest warranting disclosure in this article.

Работа поддержана Министерством высшего образования и науки Российской Федерации, проект FZZW-2023-0010.

Авторы заявляют об отсутствии конфликта интересов, требующего раскрытия в данной статье.

REFERENCES
ЛИТЕРАТУРА

1. **Wolf S., Tauber R.N.** Silicon Processing for the VLSI Era. V. 1. Process Technology. New York: Lattice Press. 2000. 416 p.
2. **Valeev A.S., Krasnikov G.Y.** Manufacturing technology of intra- and interchip interconnects for modern ULSIs: Review and concepts of development. *Russ. Microelectronics.* 2015. V. 44. N 3. P. 180-201. DOI: 10.1134/S1063739715030087.
3. **Donnelly V.M., Kornblit A.** Plasma etching: Yesterday, today, and tomorrow. *J. Vac. Sci. Technol.* 2013. V. 31. P. 050825-48. DOI: 10.1116/1.4819316.
4. **Lieberman M.A., Lichtenberg A.J.** Principles of plasma discharges and materials processing. New York: John Wiley & Sons Inc. 2005. 757 p. DOI: 10.1002/0471724254.
5. **Nojiri K.** Dry etching technology for semiconductors. Tokyo: Springer Internat. Publ. 2015. 116 p. DOI: 10.1007/978-3-319-10295-5.
6. Advanced plasma processing technology. New York: John Wiley & Sons Inc. 2008. 479 p.
7. **Standaert T.E.F.M., Hedlund C., Joseph E.A., Oehrlein G.S., Dalton T.J.** Role of fluorocarbon film formation in the etching of silicon, silicon dioxide, silicon nitride, and amorphous hydrogenated silicon carbide. *J. Vac. Sci. Technol. A.* 2004. V. 22. P. 53-60. DOI: 10.1116/1.1626642.
8. **Marra D.C., Aydil E.S.** Effect of H_2 addition on surface reactions during CF_4/H_2 plasma etching of silicon and silicon dioxide films. *J. Vac. Sci. Technol. A.* 1997. V. 15. P. 2508-2516. DOI: 10.1116/1.580762.

9. **Efremov A., Murin D., Kwon K.-H.** Concerning the Effect of Type of Fluorocarbon Gas on the Output Characteristics of the Reactive-Ion Etching Process. *Russ. Microelectronics.* 2020. V. 49. N 3. P. 157-165. DOI: 10.1134/S1063739720020031.
10. **Kimura T., Ohe K.** Model and probe measurements of inductively coupled CF_4 discharges. *J. Appl. Phys.* 2002. V. 92. P. 1780-1787. DOI: 10.1063/1.1491023.
11. **Kastenmeier B.E.E., Matsuo P.J., Oehrlein G.S.** Highly selective etching of silicon nitride over silicon and silicon dioxide. *J. Vac. Sci. Technol. A.* 1999. V. 17. P. 3179-3184. DOI: 10.1116/1.58209.
12. **Schaepkens M., Standaert T.E.F.M., Rueger N.R., Sebel P.G.M., Oehrlein G.S., Cook J.M.** Study of the SiO_2-to-Si_3N_4 etch selectivity mechanism in inductively coupled fluorocarbon plasmas and a comparison with the SiO_2-to-Si mechanism. *J. Vac. Sci. Technol. A.* 1999. V. 17. P. 26-37. DOI: 10.1116/1.582108.
13. **Efremov A.M., Murin D.B., Kwon K.-H.** Parameters of plasma and kinetics of active particles in $CF_4(CHF_3)$ + Ar mixtures of a variable initial composition. *Russ. Microelectronics*. 2018. V. 47(6). P. 371-380. DOI: 10.1134/S1063739718060033.
14. **Kimura T., Noto M.** Experimental study and global model of inductively coupled CF_4/O_2 discharges. *J. Appl. Phys.* 2006. V. 100. P. 063303 (1-9). DOI: 10.1063/1.2345461.
15. **Efremov A., Lee B.J., Kwon K.-H.** On Relationships Between Gas-Phase Chemistry and Reactive-Ion Etching Kinetics for Silicon-Based Thin Films (SiC, SiO_2 and Si_xN_y) in Multi-Component Fluorocarbon Gas Mixtures. *Materials*. 2021. V. 14. P. 1432(1-27). DOI: 10.3390/ma14061432.
16. **Lim N., Efremov A., Kwon K.-H.** A comparison of CF_4, CHF_3 and C_4F_8 + Ar/O_2 Inductively Coupled Plasmas for Dry Etching Applications. *Plasma Chem. Plasma Process*. 2021. V. 41. P. 1671-1689. DOI: 10.1007/s11090-021-10198-z.
17. **Baek S. Y., Efremov A., Bobylev A., Choi G., Kwon K.-H.** On relationships between plasma chemistry and surface reaction kinetics providing the etching of silicon in CF_4, CHF_3, and C_4F_8 gases mixed with oxygen. *Materials*. 2023. V. 16. P. 5043(1-18). DOI: 10.3390/ma16145043.
18. **Efremov A., Bobylev A., Kwon K.-H.** Concentration of fluorine atoms and kinetics of reactive-ion etching of silicon in CF_4 + O_2, CHF_3 + O_2 and C_4F_8 + O_2 mixtures. *Russ. Microelectronics.* 2023. V. 52. N 4. P. 267-275. DOI: 10.1134/S1063739723700488.
19. **Efremov A. M., Bashmakova D. E., Kwon K.-H.** Features of plasma composition and fluorine atom kinetics in CHF_3 + O_2 gas mixture. *ChemChemTech [Izv. Vyssh. Uchebn. Zaved. Khim. Khim. Tekhnol.]*. 2023. V. 66. N 1. P. 48-55.
Ефремов А.М., Башмакова Д.Е., Kwon K.-H. Особенности состава плазмы и кинетики атомов фтора в смеси CHF_3+ O_2. *Изв. вузов. Химия и хим. Технология.* 2023. Т. 66. Вып. 1. С. 48-55. DOI: 10.6060/ivkkt.20236601.6667.
20. **Shun'ko E.V.** Langmuir probe in theory and practice. Boca Raton: Universal Publ. 2008. 245 p.
21. **Lopaev D.V., Volynets A.V., Zyryanov S.M., Zotovich A.I., Rakhimov A.T.** Actinometry of O, N and F atoms. *J. Phys. D: Appl. Phys.* 2017. V. 50. P. 075202(1-17). DOI: 10.1088/1361-6463/50/7/075202.
22. **Engeln R., Klarenaar B., Guaitella O.** Foundations of optical diagnostics in low-temperature plasmas. *Plasma Sources Sci. Technol.* 2020. V. 29. P. 063001 (1-14). DOI: 10.1088/1361-6595/ab6880.
23. **Cunge G., Ramos R., Vempaire D., Touzeau M., Neijbauer M., Sadeghi N.** Gas temperature measurement in CF_4, SF_6, O_2, Cl_2, and HBr inductively coupled plasmas. *J. Vac. Sci. Technol. A.* 2009. V. 27. N 3. P. 471-478. DOI: 10.1116/1.3106626.
24. **Ho P., Johannes J.E., Buss R.J.** Modeling the plasma chemistry of C_2F_6 and CHF_3 etching of silicon dioxide, with comparisons to etch rate and diagnostic data. *J. Vac. Sci. Technol. B.* 2001. V. 19. P. 2344-2367. DOI: 10.1116/1.1387048.
25. **Hsu C.C., Nierode M.A., Coburn J.W., Graves D.B.** Comparison of model and experiment for Ar, Ar/O_2 and $Ar/O_2/Cl_2$ inductively coupled plasmas. *J. Phys. D. Appl. Phys.* 2006. V. 39. P. 3272-3284. DOI: 10.1088/0022-3727/39/15/009.
26. **Efremov A.M., Betelin V.B., Mednikov K.A., Kwon K.-H.** Plasma parameters and densities of active species in mixtures of fluorocarbon gases with argon and oxygen. *ChemChemTech [Izv. Vyssh. Uchebn. Zaved. Khim. Khim. Tekhnol.]*. 2021. V. 64. N 7. P. 46-53.
Ефремов А.М., Бетелин В.Б., Медников К.А., Kwon K.-H. Параметры плазмы и концентрации активных частиц в смесях фторуглеродных газов с аргоном и кислородом. *Изв. Вузов. Химия и хим. Технология.* 2021. Т. 64. Вып. 7. С. 46-53. DOI: 10.6060/ivkkt.20216407.6390.
27. **Efremov A.M., Smirnov S.A., Betelin V.B., Kwon K.-H.** On the comparison of reactive-ion etching mechanisms for SiO_2 in fluorine- and chlorine-containing plasmas. *ChemChemTech [Izv. Vyssh. Uchebn. Zaved. Khim. Khim. Tekhnol.]*. 2023. V. 66. N. 8. P. 52-64.
Ефремов А.М., Смирнов С.А., Бетелин В.Б., Kwon K.-H. О сравнении механизмов реактивно-ионного травления SiO_2 во фтор-и хлорсодержащей плазме. *Изв. Вузов. Химия и хим. Технология.* 2023. Т. 66. Вып. 8. С. 52-64. DOI: 10.6060/ivkkt.20236608.6746.
28. Handbook of Chemistry and Physics. Boca Raton: CRC Press. 2003. 2661 p.
29. NIST Chemical Kinetics Database. https://kinetics.nist.gov/kinetics/welcome.jsp (15.04.2024)
30. **Efremov A., Son H.J., Choi G., Kwon K.-H.** On Mechanisms Influencing Etching/Polymerization Balance in Multi-Component Fluorocarbon Gas Mixtures. *Vacuum.* 2022. V. 206. P. 111518(1-10). DOI: 10.1016/j.vacuum.2022.111518.
31. A Simple Sputter Yield Calculator. https://www2.iap.tuwien.ac.at/www/surface/sputteryield (15.04.2024).

Поступила в редакцию 16.04.2024
Принята к опубликованию 20.06.2024

Received 16.04.2024
Accepted 20.06.2024